Nitrogen pink afterglow: the mystery continues

Vasco Guerra[1], Paulo A. Sá[2] and Jorge Loureiro[1]

[1] Centro de Física dos Plasmas, Instituto Superior Técnico, 1049-001 Lisboa, Portugal
[2] Centro de Física dos Plasmas, Faculdade de Engenharia, Universidade do Porto, 4200-465 Porto, Portugal

E-mail: vguerra@ist.utl.pt

Abstract. This work extends our previous analysis of the nitrogen pink afterglow, by comparing our model predictions with the recently reported measurements of metastable $N(^2P)$ atoms and $N_2(a\ ^1\Pi_g)$ molecules. It is shown that both species reveal the presence of a characteristic maximum on their populations, occurring downstream from the discharge after an initial stage of decrease. Such behavior is a consequence of the V-V pumping-up mechanism taking place during the relaxation in the afterglow, which is followed by V-E transfers that create locally $N_2(A\ ^3\Sigma_u^+)$ and $N_2(a'\ ^1\Sigma_u^-)$ metastables.

The model predictions significantly overestimate the density of the $N_2(a\ ^1\Pi_g)$ state, revealing a problem in the description of the singlet kinetics. As singlet $N_2(a'\ ^1\Sigma_u^-)$ metastables play a crucial role in nitrogen ionization, the new results imply that the ionization mechanisms in the afterglow may have to be reviewed.

1. Introduction

In the last 10 years a considerable effort has been made to systematically characterize the pink or short-lived afterglow (SLA) in flowing nitrogen. A series of experiments performed by the teams lead by P. Supiot and N. Sadeghi have provided the emission profiles of the first positive $N_2(B\ ^3\Pi_g \rightarrow A\ ^3\Sigma_u^+)$ and first negative $N_2^+(B\ ^2\Sigma_u^+ \rightarrow X\ ^2\Sigma_g^+)$ systems, as well as the absolute concentrations of $N_2(A\ ^3\Sigma_u^+)$, $N(^4S)$ atoms and electrons in a nitrogen flowing afterglow [1]–[5]. These studies have revealed the formation of peaks for the electron density and for the densities of the radiative states $N_2(B\ ^3\Pi_g)$ and $N_2^+(B\ ^2\Sigma_u^+)$ and metastables $N_2(A\ ^3\Sigma_u^+)$, which occur in a region where the electric field is negligible, downstream from the discharge and after a dark zone [*cf.* figure 2 below].

The energy state diagram of N_2 and N_2^+ is shown in figure 1. The nitrogen molecule has two manifolds of electronic states, which are somewhat independent. The triplet manifold includes, among others, the metastable state $N_2(A\ ^3\Sigma_u^+)$ (marked in blue), and the radiative states $N_2(B\ ^3\Pi_g)$ (shown in green) and $N_2(C\ ^3\Pi_u)$. The latter two states give raise to the emissions of the first and second positive systems of nitrogen. The singlet manifold encompasses the metastable states $N_2(a'\ ^1\Sigma_u^-)$ (indicated in red), $N_2(a\ ^1\Pi_g)$ and $N_2(w\ ^1\Delta_u)$. As discussed below, the low-laying metastable states of both manifolds, $N_2(A\ ^3\Sigma_u^+)$ and $N_2(a'\ ^1\Sigma_u^-)$, are important energy reservoirs and play a significant role in the explanation of the phenomenon. The pink emission, which gives its name to the SLA, comes from the first negative system of nitrogen, clearly identified in the figure.

In parallel with the experimental studies, a detailed kinetic model has been developed in order to interpret and predict the experimental measurements. Details about the theoretical

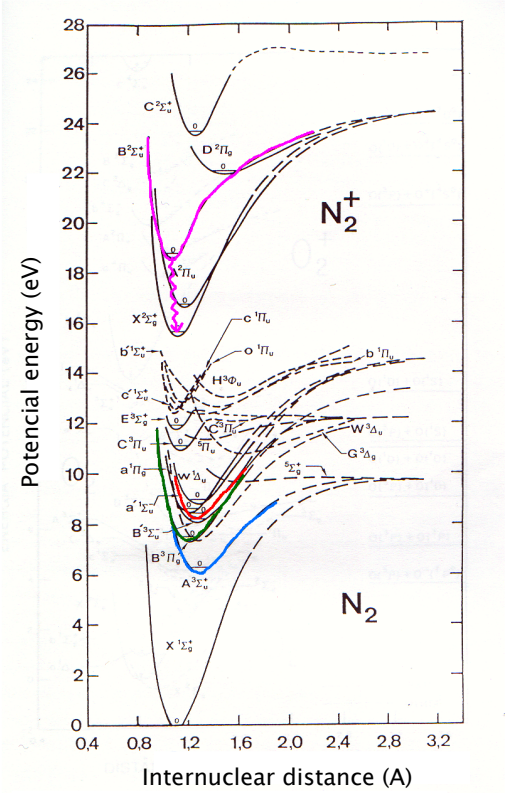

Figure 1. Energy state diagram of N_2 and N_2^+. The pink emission corresponds to the transition $N_2^+(B\ ^2\Sigma_u^+ \rightarrow X\ ^2\Sigma_g^+)$.

model can be found in [6]–[8]. The theoretical investigation allowed to solve the puzzle to a big extent, by unambiguously showing that vibrationally excited molecules in high v levels are in the origin of the peaks observed in the flowing afterglow for the concentrations of various species, as a consequence of the so-called V-V pumping-up mechanism. As a matter of fact, the anharmonicity of the potential curve of $N_2(X\ ^1\Sigma_g^+)$ implies that the energy difference between neighboring vibrational levels decreases from the bottom to the top of the vibrational ladder. As a consequence, the vibration-vibration (V-V) reactions

$$N_2(X,v) + N_2(X,w) \leftrightarrow N_2(X,v-1) + N_2(X,w+1) \tag{1}$$

are not exactly resonant and, for $v < w$, have a larger coefficient for the forward process. This originates a climbing in the vibrational ladder during the relaxation process in the afterglow [9]. The highly vibrationally excited dark states $N_2(X\ ^1\Sigma_g^+, v)$ formed in this way subsequently transfer their energy to electronically excited states through vibration-electronic (V-E) energy transfer processes that can be mediated by heavy-particles (such as $N(^4S)$ atoms) and/or electrons [8, 10, 11]. The key point is the formation of $N_2(A\ ^3\Sigma_u^+)$ and $N_2(a'\ ^1\Sigma_u^-)$ locally in the afterglow, which are then involved in a series of reactions of formation of other species [7, 8].

In this work we extend our previous results to the analysis of the recent measurements of the absolute concentrations of $N(^2P)$ and $N_2(a\ ^1\Pi_g)$ metastables in the nitrogen afterglow

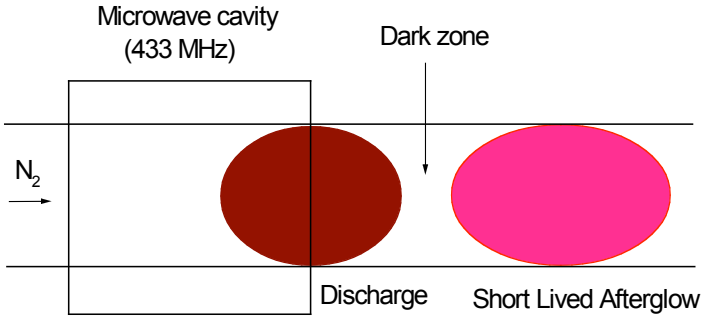

Figure 2. Schematic description of the nitrogen flowing afterglow under investigation, showing the active discharge, the dark zone and the SLA.

reported in[12], which were obtained using a complex technique based on emission spectroscopy. The system under analysis is the afterglow of a surface-wave discharge operating at frequency $\omega/2\pi = 433$ MHz, pressure $p = 3.3$ Torr, in a Pyrex tube of inner radius $R = 1.9$ cm, as schematically depicted in figure 2. The electron density at the end of the discharge/beginning of the post-discharge is estimated to be $n_e(0) = 3 \times 10^{10}$ cm^{-3} [1], a value slightly larger than the critical value for a surface-wave propagating at 433 MHz, $n_{ec} \simeq 1.3 \times 10^{10}$ cm^{-3}, and the value of the gas temperature in the discharge is approximately 1000 K. These afterglow conditions correspond to the experimental characterization from [1]–[5], which allows a detailed comparison between the model predictions and the experimental measurements. For these conditions, the calculated effective field in the discharge is $E_e/N = 4.6 \times 10^{-16}$ V.cm^2 and the vibrational temperature of ground-state molecules, T_V, is about 6200 K. Take notice that the critical density for surface-wave propagation is calculated for the homogeneous collisionless case from $n_{ec} = n_c(1 + \varepsilon_d)$, where $n_c = m\varepsilon_0\omega^2/e^2$ is the cutoff plasma density, m and e denoting the electron mass and charge, respectively, and ε_d is the relative permittivity of Pyrex [13]. However, electron densities below n_{ec} have been experimentally observed in surface wave discharges, as a consequence of the effects of collisions and of the inhomogeneity in the spatial distribution of the plasma density [14].

2. Kinetic model

The Kinetic model is described in detail in [7]. It comprises two modules, one describing the stationary discharge in the alternating field and another one the afterglow. The first module allows the calculation of the electron energy distribution function, the vibrational distribution function (VDF) of $N_2(X\ ^1\Sigma_g^+, v)$ molecules, the concentrations of N_2 excited states $A\ ^3\Sigma_u^+$, $B\ ^3\Pi_g$, $B'\ ^3\Sigma_u^-$, $C\ ^3\Pi_u$, $a'\ ^1\Sigma_u^-$, $a\ ^1\Pi_g$, $w\ ^1\Delta_u$, of $N(^4S)$ ground-state and excited ^2D and ^2P atoms, as well as of $N_2^+(X\ ^2\Sigma_g^+$, $B\ ^2\Sigma_u^+)$ and N_4^+ ions. The system of coupled equations includes the stationary homogeneous electron Boltzmann equation, the rate balance equations for the neutral and charged heavy-particles and the quasi-neutrality condition. The maintenance high frequency field is self-consistently determined by requiring an exact equality between the total rate of ionization and the total rate of electron losses. A list with all the reactions considered in the model, together with their corresponding rate coefficients, can be found in [7].

Once the steady-state discharge concentrations and distributions have been obtained, the relaxation model for the post-discharge is basically the same as in the discharge, by considering time-dependent equations with zero electric field and the discharge calculated values as initial conditions for the afterglow. It is worth remarking that the treatment is time-dependent and space-homogeneous (0-D). As the experimental data refers to space profiles, in order to compare the model predictions with the experimental measurements it is necessary to translate afterglow time into afterglow distance by means of the mass flow and the experimental gas temperature profile in the post-discharge.

As largely discussed in [6]–[8], the critical issue to understand the nitrogen afterglow is the local formation of the metastable states $N_2(A\ ^3\Sigma_u^+)$ and $N_2(a'\ ^1\Sigma_u^-)$, in V-E transfers that follow the V-V pumping-up process. Assuming these transfers to be induced by heavy-particles, one possible mechanism is via reactions [6]–[8]

$$N_2(X, v \geq 39) + N(^4S) \rightarrow N_2(A) + N(^2D) \tag{2}$$

$$N_2(X, v \geq 38) + N(^4S) \rightarrow N_2(a') + N(^4S)\ . \tag{3}$$

Once these two metastable states are created, other species are readily created. Thus, $N_2(B\ ^3\Pi_g)$ is formed through

$$N_2(A) + N_2(X, 5 \leq v \leq 14) \rightarrow N_2(B) + N_2(X, v = 0)\ . \tag{4}$$

On the other hand, electrons and $N_2{}^+(X\ ^2\Sigma_g^+)$ ions are formed by the Penning mechanisms

$$N_2(A) + N_2(a') \rightarrow N_2{}^+ + N_2 + e \tag{5}$$

and

$$N_2(a') + N_2(a') \rightarrow N_2{}^+ + N_2 + e\ . \tag{6}$$

Finally, $N_2{}^+(B\ ^2\Sigma_u^+)$ ions are formed by

$$N_2(X, v \geq 12) + N_2{}^+(X) \rightarrow N_2{}^+(B) + N_2(X)\ . \tag{7}$$

This set of reactions provides a satisfactory explanation for the concentrations and profiles of electrons and excited states $N_2(A\ ^3\Sigma_u^+,\ B\ ^3\Pi_g)$ and $N_2{}^+(B\ ^2\Sigma_u^+)$ [6].

The possible role of electron mediated V-E energy transfers was verified in [7] by assuming, as an alternative to reactions (2) and (3), that electronically excited states can be created by reactions

$$e + N_2(X, v \geq 25) \rightarrow e + N_2(A) \tag{8}$$

and

$$e + N_2(X, v \geq 38) \rightarrow e + N_2(a')\ , \tag{9}$$

and will not be discussed here. Nevertheless, it is worth noting that the recent experiments reported in [10, 11] show beyond doubt that electron mediated V-E processes occur in CO, at ionization degrees as low as 10^{-9}–10^{-7}. For this reason we suggested in [6] and confirmed in [7] that resonant electron mediated vibration-electronic V-E energy transfers may contribute as well to the formation of electronically excited states in the nitrogen afterglow. In fact, the reactions of associative or Penning ionization that occur in the post-discharge can create low energy electrons able to participate nearly isoenergetic reactions. Moreover, the depopulation of high vibrational levels $N_2(X\ ^1\Sigma_g^+, v)$ by electron superelastic collisions may substantially increase the energy of these electrons.

3. Results and discussion

Figure 3 shows the vibrational distribution function (VDF) of $N_2(X\ ^1\Sigma_g^+, v)$ molecules calculated at different afterglow times between 0 and 1 s, clearly illustrating the V-V pumping of the high v levels. The tail of the VDF passes through a maximum for afterglow times of the order of 10^{-2} s, which starts to exist for levels $v \geq 25$ and is very pronounced for $v \geq 35$. The open circles are the Raman scattering measurements in the afterglow of a surface-wave discharge corresponding to the conditions of the calculations, for an afterglow time $t \sim 5 \times 10^{-2}$ s [15]. The black circle is the cavity ringdown spectroscopy measurement of the population of level $v = 18$ in a DC discharge at $p = 2.3$ Torr and $I = 100$ mA [16], which is, to our knowledge, the only measurement available for a relatively high vibrational level. Notice that the presence of these dark high vibrational levels in the SLA, which are not effectively populated in the discharge, makes them available to participate in chemical V-E reactions in the afterglow. They are thus the energy carriers responsible for most of the effects observed in the afterglow, including the raise in the populations of several species. The contribution of ground-state atoms $N(^4S)$ to the formation of the SLA via three-body recombination has also been suggested in the literature [1, 17]. However, it seems clear that this mechanism, although with a possible contribution to the absolute concentrations of the different species experimentally found, cannot by itself justify the overall behaviour of the nitrogen afterglow [8].

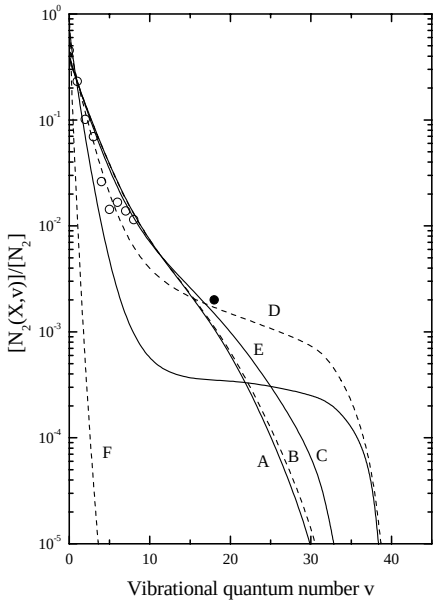

Figure 3. VDF of $N_2(X\ ^1\Sigma_g^+, v)$ molecules in the nitrogen afterglow of a $\omega/2\pi = 433$ MHz discharge at $p = 3.3$ Torr, in a cylindrical tube of inner radius $R = 1.9$ cm, for which $E_e/N = 4.6 \times 10^{-16}$ V.cm^2 and $T_V \simeq 6200$ K, at different instants in the afterglow: $t = 0$ (A); $t = 10^{-4}$ s (B); $t = 10^{-3}$ s (C); $t = 10^{-2}$ s (D); $t = 10^{-1}$ s (E); and $t = 1$ s (F). Experimental data from [15] (○) and [16] (●) (see text).

The excellent agreement obtained between our model calculations and the experimental results for the population of the $N_2(A\ ^3\Sigma_u^+)$ is shown in figures 4. The theoretical results correspond to the kinetic scheme delineated above. This agreement extends to the populations of states $N_2(B\ ^3\Pi_g)$ and $N_2{}^+(B\ ^2\Sigma_u^+)$, to ground state $N(^4S)$ atoms and to the electron density [6]–[8].

The comparison of further model predictions with the recently measured populations of $N(^2P)$ and $N_2(a\ ^1\Pi_g)$ constitutes an important test to verify the validity of the adopted kinetic scheme.

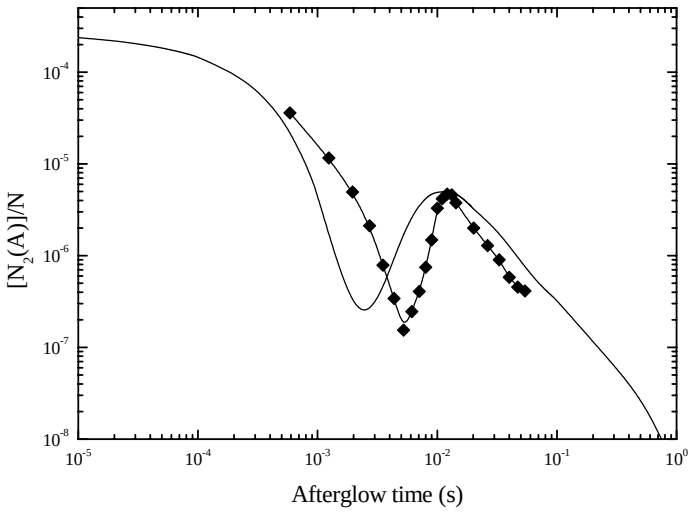

Figure 4. Measured [4] and calculated absolute population of $N_2(A\ ^3\Sigma_u^+)$ metastables along the afterglow, for the conditions of figure 3.

The kinetics of $N(^2P)$ metastables is strongly coupled to the kinetics of ground-state $N(^4S)$ atoms and triplet $N_2(A\ ^3\Sigma_u^+)$ molecules. In fact, in a nitrogen post-discharge $N(^2P)$ atoms are essentially formed and destroyed in reactions involving these two species [6, 7], namely

$$N_2(A) + N(^4S) \rightarrow N_2(X, 6 \leq v \leq 9) + N(^2P) \tag{10}$$

and

$$N_2(X, v \geq 10) + N(^2P) \rightarrow N_2(A) + N(^4S)\ . \tag{11}$$

Figure 5 reveals that the excellent agreement between the model predictions and the measurements previously found for the populations of $N_2(A\ ^3\Sigma_u^+)$, $N_2(B\ ^3\Pi_g)$ and $N(^4S)$ during the afterglow is also extended to $N(^2P)$ atoms. The very good accordance of the theoretical predictions with the experimental results is a strong confirmation of the correctness of our description of the elementary processing ruling the atomic, vibrational and triplet kinetics.

The situation with the singlet kinetics seems to be different. During the relaxation in the afterglow, the population of $N_2(a\ ^1\Pi_g)$ metastables is mainly determined by reactions

$$N_2(a) + N_2 \leftrightarrow N_2(a') + N_2\ . \tag{12}$$

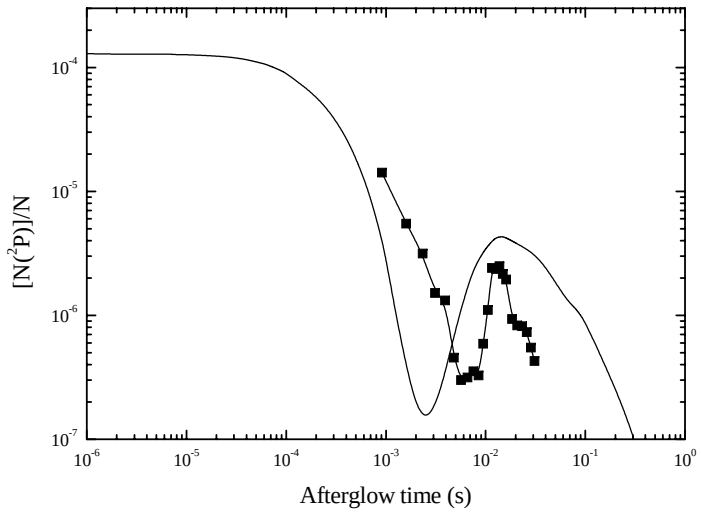

Figure 5. Measured [12] and calculated absolute population of N(^2P) metastables along the afterglow, for the conditions of figure 3.

The well known Lyman-Birge-Hopfield emission $a\ ^1\Pi_g$–$X\ ^1\Sigma_g^+$ contributes at most about 10% for the destruction of the singlet $N_2(a\ ^1\Pi_g)$. At $p = 3.3$ Torr and without an external field, the populations of $N_2(a'\ ^1\Sigma_u^-)$ and $N_2(a\ ^1\Pi_g)$ metastables should be approximately in equilibrium. Hence, it is expected that the concentrations of both states exhibit a similar profile along the post-discharge. $N_2(a\ ^1\Pi_g)$ should then follow $N_2(a'\ ^1\Sigma_u^-)$ and present the characteristic profile of a raise in the afterglow after a minimum corresponding to the position of the dark zone. For the $N_2(a'\ ^1\Sigma_u^-)$ state this is a direct consequence of the V-V pumping-up together with reaction (3), whereas $N_2(a\ ^1\Pi_g)$ is coupled to this state through reactions (12). Figure 6 confirms this profile is indeed obtained for the concentration of singlet $N_2(a\ ^1\Pi_g)$ metastables, both theoretically (full curve) and experimentally (data points, taken from [12]). However, there is a disagreement of about two orders of magnitude between the calculated and measured concentrations, the calculations overestimating the measurements reported in [12]. The peak value of the calculated relative concentration of $N_2(a\ ^1\Pi_g)$ molecules is close to 9×10^{-8}, whereas the one for $N_2(a'\ ^1\Sigma_u^-)$ is about 2×10^{-5} (the ratio of both densities is therefore about a factor of 220, *i.e.*, very close to equilibrated populations, see below).

It is worth to stress that the present kinetic model has been tested and validated by comparing the calculated data with experimental measurements in many different discharge and post-discharge situations. Hence, any attempt to reconcile the calculations and measurements shown in figure 6 should not change the other quantities already calculated in the afterglow, nor the ionization balance (and thus the concentration of singlet $N_2(a'\ ^1\Sigma_u^-)$ metastables) in the discharge.

In principle, the overestimation of the relative concentration of $N_2(a\ ^1\Pi_g)$ state in the model is related either to an overestimation of its creation mechanisms or to an underestimation of its destruction processes. Let us concentrate first on the later scenario. Destruction in the forward reaction (12) is of course not very effective, due to the reverse process which redistributes the

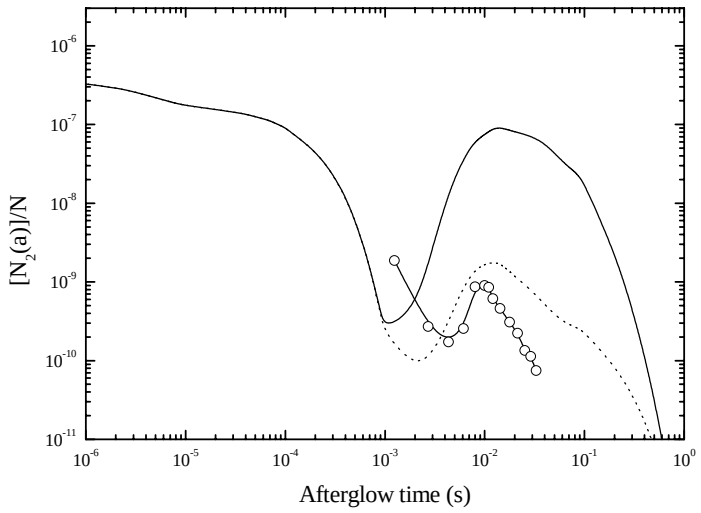

Figure 6. Measured [12] and calculated (full curves) absolute population of $N_2(a\ ^1\Pi_g)$ metastables along the afterglow, for the conditions of figure 3. The dashed curves are obtained from the model by lowering the rate coefficient of process (3).

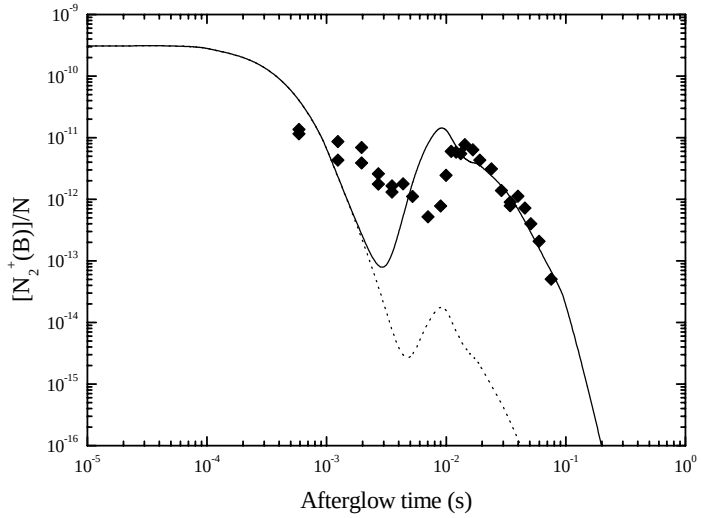

Figure 7. Measured [12] and calculated absolute population of $N(^2P)$ metastables along the afterglow, for the conditions of figure 3, with the same notation as in figure 6.

newly formed $N_2(a'\ ^1\Sigma_u^-)$ molecules and ensures almost equilibrated populations of both states (this means $[N_2(a, v = 0)]/[N_2(a', v = 0)] \sim 1/200$ at 350 K). The direct reaction $N_2(a) + N_2 \rightarrow$ (*products*) proceeds with a rate coefficient of 2×10^{-11} cm^3/s. Although the reaction products of the forward reaction (12) have not been identified and a priori may include any of the states $X\ ^1\Sigma_g^+$, $A\ ^3\Sigma_u^+$, $B\ ^3\Pi_g$ and $W\ ^3\Delta_u$ in addition to $N_2(a'\ ^1\Sigma_u^-)$ [18], which would decrease the total population of the singlet states, the rate coefficient for the total quenching from the singlet manifold by N_2 has been determined to be of the order of 2×10^{-13} cm^3/s [19, 20]. Therefore, the quenching of $N_2(a\ ^1\Pi_g)$ in reaction (12) must indeed give $N_2(a'\ ^1\Sigma_u^-)$. Another possibility is the destruction of singlet metastables in collisions with $N(^4S)$ atoms. Notice that the similar reaction (10) involving the triplet metastable $N_2(A\ ^3\Sigma_u^+)$ is very efficient. To our knowledge such a reaction is not found in the literature for the singlet states. Nevertheless we have checked if it could influence the calculated populations of $N_2(a\ ^1\Pi_g)$ in the afterglow. Considering a rate coefficient of 10^{-11} cm^3/s for the quenching by $N(^4S)$ atoms, the peak of the relative population of $N_2(a\ ^1\Pi_g)$ metastables decreases only by a factor of 2. That being so, extra sources of destruction of $N_2(a\ ^1\Pi_g)$ state seem difficult to justify.

From the side of production of $N_2(a\ ^1\Pi_g)$ state, its major source is yet the reverse reaction (12), three-body recombination being always negligible for the present conditions. Therefore, if $N_2(a'\ ^1\Sigma_u^-)$ state is not formed through process (3) as efficiently as proposed in [6, 7], then a better agreement between calculations and measurements is possible for the former state. This is shown by the dotted curves in figure 6, obtained lowering the rate coefficient of process (3). This assumption does not affect the populations calculated under discharge conditions, nor the concentrations of the different triplet and atomic states during the afterglow. However, it dramatically influences the concentration of electrons and ions in the afterglow, since $N_2^+(B\ ^2\Sigma_u^+)$ ions and electrons are produced in the afterglow through reactions (5) and (6). This is evident from the dotted curve in figure 7. In this case, extra ionization sources are required to explain the ionization degree experimentally observed in the afterglow. These additional sources may be related to ionization processes involving highly vibrationally excited molecules.

Early attempts to explain ionization in nitrogen discharges involving vibrationally excited ground state molecules were made in [21]–[23]. In particular, reactions

$$N_2(X\ ^1\Sigma_g^+, v \geq 32) + N_2(X\ ^1\Sigma_g^+, v \geq 32) \rightarrow {N_4}^+ + e \tag{13}$$

and

$$N_2(a''\ ^1\Sigma_g^+) + N_2(X\ ^1\Sigma_g^+, v \geq 13) \rightarrow {N_4}^+ + e \tag{14}$$

were proposed. However, for discharge conditions the VDF of ground-state nitrogen molecules is generally not strong enough populated in the high vibrational levels to allow reactions (13) to be efficient. Moreover, the metastable state $N_2(a''\ ^1\Sigma_g^+)$ is strongly quenched by N_2 [24] and the relative population of this state is always very low. Thus, process (14) cannot contribute significantly to ionization. Notice as well that reaction (13) was retracted [23], where it has been suggested it could somehow be an effective representation of a sequence of other elementary steps.

Although mechanisms involving highly vibrationally excited $N_2(X\ ^1\Sigma_g^+)$ molecules have been unambiguously ruled out for discharge conditions [7], their possible existence in the post-discharge (after the pumping-up of high vibrational levels) may be reanalyzed. In particular, reactions such as

$$N_2(X\ ^1\Sigma_g^+, v \geq 30) + N_2(a'\ ^1\Sigma_u^-) \rightarrow N_2(X\ ^1\Sigma_g^+) + {N_2}^+ + e \tag{15}$$

and

$$N_2(X\ ^1\Sigma_g^+, v \geq 36) + N_2(B\ ^3\Pi_g) \rightarrow N_2(X\ ^1\Sigma_g^+) + {N_2}^+ + e\ , \tag{16}$$

may have to be reconsidered. For the rate coefficients usually reported in the literature for these processes, they do not seem too promising *a priori* [6]. Nevertheless, work is in progress to clarify the issue.

4. Conclusions

The recent measurements of the absolute concentrations of $N(^2P)$ atoms and $N_2(a\ ^1\Pi_g)$ molecules [12] motivated a theoretical investigation of the elementary processes determining the kinetics of both states. Such study was made with the help of the models developed in [7, 8]. It is shown that both species reveal the presence of a characteristic maximum on their populations, occurring downstream from the discharge after an initial stage of decrease. This behavior is a result of the V-V pumping-up effect which populates the high vibrational levels of ground-state $N_2(X\ ^1\Sigma_g^+)$ molecules during the afterglow. These levels are subsequently involved in V-E energy transfer processes responsible for the local formation of $N_2(A\ ^3\Sigma_u^+)$ and $N_2(a'\ ^1\Sigma_u^-)$ metastables in the post-discharge.

The very good agreement obtained for the concentration of $N(^2P)$ atoms supports the correctness of the present description of the atomic, vibrational and triplet kinetics and confirms the strong coupling between the kinetics of $N(^4S)$ and $N(^2P)$ atoms and $N_2(A\ ^3\Sigma_u^+)$ molecules. However, the model predictions significantly overestimate the density of the $N_2(a\ ^1\Pi_g)$ state, which can be a consequence of an overestimation of the efficiency of the V-E transfer leading to the formation of singlet $N_2(a'\ ^1\Sigma_u^-)$ metastables. If this is the case, then the ionization mechanisms in the afterglow may have to be reviewed. The "mystery" [17] continues.

Acknowledgments

We are indebted to Professors Philippe Supiot, Corinne Foissac and Nader Sadeghi, for several very fruitfull discussions.

References

[1] N. Sadeghi, C. Foissac, and P. Supiot. Kinetics of $N_2(A\ ^3\Sigma_u^+)$ molecules and ionization mechanisms in the afterglow of a flowing N_2 microwave discharge. 2001 *J. Phys. D: Appl. Phys.* **34** 1779–1788.

[2] D. Blois, P. Supiot, M. Barj, A. Chapput, C. Foissac, O. Dessaux, and P. Goudmand. The microwave source's influence on the vibrational energy carried by $N_2(X\ ^1\Sigma_g^+)$ in a nitrogen afterglow. 1998 *J. Phys. D: Appl. Phys.* **31** 2521–2531.

[3] S. Mazouffre, R. Engelm, P. Vankan, D. Schram, C. Foissac, P. Supiot, and N. Sadeghi. Density and temperature of N atoms in the afterglow of a microwave discharge measured by two-photon laser induced fluorescence technique. 2001 *Plasma Sources Sci. Technol.* **10** 168–175.

[4] E. Eslami, C. Foissac, A. Campargue, P. Supiot, and N. Sadeghi. Vibrational and rotational distributions in $N_2(A\ ^3\Sigma_u^+)$ metastable state in the short-lived afterglow of a flowing nitrogen microwave plasma. In *XVIth Europhysics Conference on Atomic and Molecular Physics of Ionized Gases (ESCAMPIG) – 5th International Conference on Reactive Plasmas (ICRP) Joint Meeting*, volume 1, pages 57–58, Grenoble, France, 2002. European Physical Society.

[5] E. Eslami, A. Campargue, C. Foissac, P. Supiot, and N. Sadeghi. Characterization of long-lived species in the afterglow of nitrogen microwave discharge. In *Frontiers in Low Temperature Plasma Diagnostics (FLTPD-V)*, page 213, Villaggio Cardigliano, Specchia (Lecce), Italy, 2003.

[6] P. A. Sá, V. Guerra, J. Loureiro, and N. Sadeghi. Self-consistent kinetic model of the short-lived afterglow in flowing nitrogen. 2004 *J. Phys. D: Appl. Phys.* **37** 221–231.

[7] V. Guerra, P. A. Sá, and J. Loureiro. Kinetic modeling of low-pressure nitrogen discharges and post-discharges. 2004 *Eur. Phys. J. Appl. Phys.* **28** 125–152.

[8] J. Loureiro, P. A. Sá, and V. Guerra. On the difficulty of $N(^4S)$ atom recombination to explain the appearance of the pink afterglow in a n_2 flowing discharge. 2006 *J. Phys. D: Appl. Phys.* **39** 122–125.

[9] C. E. Treanor, J. W. Rich, and R. G. Rehm. Vibrational relaxation of anharmonic oscillators with exchange-dominated collisions. 1968 *J. Chem. Phys.* **48** 1798–1807.

[10] E. Plönjes, P. Palm, J. W. Rich, I. V. Adamovich, and W. Urban. Electron-mediated vibration-electronic (V-E) energy transfer in optically pumped plasmas. 2002 *Chem. Phys.* **279** 43–54.

[11] Yu. G. Utkin, I. V. Adamovich, and J. W. Rich. Time-resolved measurements of ionization and vibration-to-electronic energy transfer in optically pumped plasmas. 2005 *J. Phys. D: Appl. Phys.* **38** 688–696.

[12] E. Eslami, C. Foissac, P. Supiot, and N. Sadeghi. Determination of the absolute density of $N(^2P)$ metastable atoms and $N_2(a\ ^1\Pi_g)$ molecules in a flowing nitrogen mivrowave discharge. In V. Ciupina, G. Musa, and R. Vladoiu, editors, *XVIIth Europhysics Conference on Atomic and Molecular Physics of Ionized Gases (ESCAMPIG)*, page 197, Constanţa, Romania, Romania, 2004. European Physical Society.

[13] I. P. Ganashev and H. Sugai. Surface-wave propagation along a corrugated plasma-dielectric surface. 2005 *Surf. Coat. Thechnol.* **200** 792–795.
[14] F. M. Dias, E. Tatarova, and C. M. Ferreira. Spatially resolved experimental investigation of a surface wave sustained discharge in nitrogen. 1998 *J. Appl. Phys.* **83** 4602–1235.
[15] P. Supiot, D. Blois, S. D. Benedictis, G. Dilecce, M. Barj, A. Chapput, O. Dessaux, and P. Goudmand. Excitation of $N_2(B\ ^3\Pi_g)$ in the nitrogen short-lived afterglow. 1999 *J. Phys. D: Appl. Phys.* **32** 1887–1893.
[16] P. Macko, G. Cunge, and N. Sadeghi. Density of $N_2(X\ ^1\Sigma_g^+, v = 18)$ molecules in a dc glow discharge measured by cavity ringdown spectroscopy at 227 nm; validity domain of the technique. 2001 *J. Phys. D: Appl. Phys.* **34** 1807–1811.
[17] N. Sadeghi. Mistery of nitrogen pink afterglow. In *XXVII International Conference on Phenomena in Ionized Gases (ICPIG)*, Eindhoven, The Netherlands, 2005.
[18] W. J. Marinelli, W. J. Kessler, B. D. Green, and W. A. M. Blumberg. Quenching of $N_2(a\ ^1\Pi_g,\ v' = 0)$ by N_2, O_2, CO, CO_2, CH_4, H_2, and Ar. 1989 *J. Chem. Phys.* **90** 2167–2173.
[19] W. J. Marinelli, B. D. Green, M. A. de Faccio, and W. A. M. Blumberg. Vibrational relaxation and intersystem crossing in $N_2(a\ ^1\Pi_g,\ v' = 0)$. 1988 *J. Phys. Chem.* **92** 3429–3237.
[20] H. Umemoto, R. Ozeki, M. Ueda, and M. Oku. Reactions of $N_2(a'\ ^1\Sigma_-^1)$ with H_2, CH_4, and their isotopic variants: Rate constants and the production yields of H(D) atoms. 2002 *JChemPhys* **117** 5654–5659.
[21] L. S. Polak, P. A. Sergeev, and D. I. Slovetskii. Nitrogen ionization mechanism in a glow discharge. 1977 *High Temp.* **15** 13–20.
[22] Yu. B. Golubovskii and V. M. Telezhko. Ionization processes in a nitrogen discharge at medium pressures. 1984 *High Temp.* **22** 340–348.
[23] L. G. Bol'shakova, Yu. B. Golubovskii, V. M. Telezhko, and D. G. Stoyanov. Mechanism for ionization of nitrogen molecules in self-sustained discharges. 1990 *Sov. Phys. Tech. Phys.* **35** 665–668.
[24] A. B. Wedding, J. Borysow, and A. V. Phelps. $N_2(a''\ ^1\Sigma_g^+)$ metastable collisional destruction and rotational excitation transfer by N_2. 1993 *J. Chem. Phys.* **98** 6227–6234.